Photonic synthesis of THz signals (invited paper)

A. J. Seeds (1), C. C. Renaud (1), M. Pantouvaki (1), M. Robertson (2), I. Lealman (2), D. Rogers (2), R. Firth (2), P. J. Cannard (2), R. Moore (2), R. Gwilliam (3)

1 : Photonics Group, Dept of Electronic and Electrical Engineering, University College London, Torrington Place, London WC1E 7JE, UK, Tel: +44(0)20 7679 7928, Fax +44(0)20 7388 9325 email: a.seeds@ee.ucl.ac.uk

2 : Centre For Integrated Photonics, Ipswich, IP5 3RE, UK

3 : University of Surrey, Guildford Surrey GU2 7RX, UK

***Abstract* — In this paper we present a review of our work on photonic synthesis of high spectral purity THz signals. This work includes novel developments on optical frequency comb generation (integrated, 2THz span, 25 GHz spacing), frequency locking of semiconductor lasers (1kHz channel stability, 10 ns switching time) and high speed photodetectors integrated with antennas (3dB bandwidth >108 GHz, 0.2 A/W responsivity , 148 µW output power at 457 GHz).**

***Index Terms* — Photodetector, millimetre-wave, THz source, heterodyne source, semiconductor laser.**

I. Introduction

Currently, the most widely used approach to THz signal generation is the detection of femtosecond optical pulses using low temperature grown photoconductors [1]. Whilst this approach is attractive for its wideband capability (upper frequency limit > 5 THz) output power at specific frequencies is low (< 1 µW) and detection sensitivity is restricted because of the pulsed nature of the source and its limited spectral purity, resulting from source laser jitter. The invention of the Uni-travelling Carrier (UTC) detector at NTT laboratories [2] has opened the route to efficient photodetection at the lower (< 2 THz) frequencies and has inspired us to work on photonic techniques for high spectral purity, continuous wave (CW) generation of THz signals. Our approach is based on generating a comb of optical frequencies which are highly correlated and spaced by a supplied precisely defined microwave frequency, selecting comb lines separated by the desired THz frequency using semiconductor laser locking techniques and then converting the photonic heterodyne signal into a THz signal using an ultra-fast photodiode detector, integrated with THz antenna. In this paper we present the technologies we have developed to implement this approach and illustrate them with current results.

II. Optical Frequency Comb Generation (OFCG)

Several solutions have been proposed to provide a regularly spaced frequency comb, such as a Fabry-Perot interferometer or a fibre ring resonator [3]. Unfortunately the frequency accuracy and stability of these devices are limited by the optical length of the resonators. Another solution is the use of deep angle modulation of an optical source to generate precisely spaced frequency lines [4]. However the number of frequency lines and their spacing are limited by the difficulty of realising such modulation at high frequencies. Other solutions such as an amplified fibre loop comb generator [5] or mode locked semiconductor lasers [6] can offer hundreds of lines with a spacing from 10 to 25 GHz over a band of at least 1THz.

The principle of the FM laser [7] avoids the strong intensity modulation associated with the mode-locked laser solution and offers a large number of equally spaced frequency lines, spaced by the FM source frequency, over the gain spectrum of the semiconductor laser. In previous work we have realised such a laser using the Quantum Confined Stark Effect (QCSE) as the refractive index modulation mechanism, first in the GaAs/AlGaAs based material (850 nm wavelength) [8], and, more recently, in an external cavity InP based laser [9].

In our latest work we have fabricated a monolithic FM laser using 8 quantum well quaternary/quaternary InP/InGaAsP material. The peak photoluminescence wavelength was 1548 nm. Shallow ion implantation was used to generate quantum well intermixing (QWI) to realise low loss phase and modulation sections, based on the technology described in [10]. After implantation the wafer was rapidly thermally processed at 650 °C for 90 seconds which created a 30 nm blue-shift of the bandgap in the modulator section. The fabricated laser was a ridge waveguide design with oxide-bridged contacts in order to reduce the capacitance of the modulator section. It had a 1.5 mm long gain section, a 170 µm long phase section and a 170 µm long modulation section. The sections were separated by an isolation trench. The oxide-bridged contact for the modulation section gave a 380 fF measured capacitance. As both phase section and modulation section were intermixed, the laser threshold remained relatively low at 70 mA for a 1.88 mm long device. The laser was operated at 250 mA bias current giving a total output of 6 mW coupled in a single mode fibre.

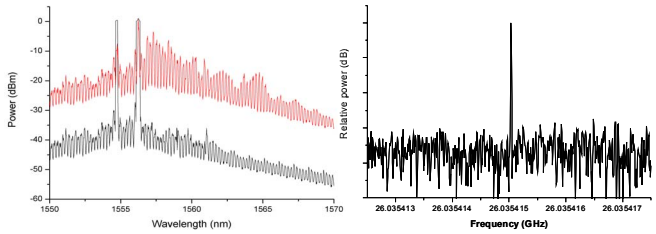

Fig. 1. Output spectrum of the FM laser when modulated (upper trace) and not (lower trace) (left), Detected heterodyne spectrum of two adjacent lines (right)

The output of the laser was split between two measurement systems. One was an optical spectrum analyser and the other used an erbium doped fibre amplifier (EDFA), two couplers and 0.6 nm bandwidth filters to measure the heterodyne between two adjacent comb lines in order to check their relative stability and frequency relation to the modulation source. The output of the laser was also monitored using a digital communications analyser with 65 GHz bandwidth photodetector to observe any residual intensity modulation.

Fig. 1 (left) shows the output spectrum of the device with and without 26 GHz modulation at power level 26 dBm (with -2 V bias) applied. With no modulation lasing was on two different longitudinal modes. With modulation the spectrum shows a large number of lines with less than 30 dB extinction to the main peak compared to a side mode suppression ratio of about 40 dB when the laser was operating without modulation. The comb span for lines of power > -30 dBm exceeds 2.5 THz.

To complete the measurement, we measured the heterodyne between two adjacent lines of the comb. The result is shown in Fig. 1 (right) for one given pair of lines. For this measurement the spectrum analyser span was 5 kHz and the resolution bandwidth was 10 Hz. The line was at the exact frequency of the modulating source and had the same spectral purity as was expected. Furthermore when measured on the digital oscilloscope the laser did not show measurable intensity modulation, thus confirming the FM operation.

III. Optical Injection Phase Lock Loop

In order to create highly stable heterodyne frequency, the two lines to be heterodyned should be highly correlated and stable. Furthermore, to create a tuneable source the filter system for the comb lines should also be agile. The solution for such filters we have adopted uses tuneable lasers locked to the master comb source. This allows both stable line selection and agility. To lock the laser two techniques could be used. The optical injection locking technique (OIL) offers the advantage of exact and quasi-instantaneous locking to one of the comb lines, however as the locking bandwidth is narrow it does not offer long term locking stability. By contrast, the optical phase lock loop (OPLL) can provide a larger locking bandwidth, however the maximum acceptable loop delay will be limited by the laser linewidth (about 1ns for a typical DFB laser). Therefore, integration is required for successful implementation. We have overcome these limitations by combining injection locking and phase locking in an optical injection phase lock loop (OIPLL) [11].

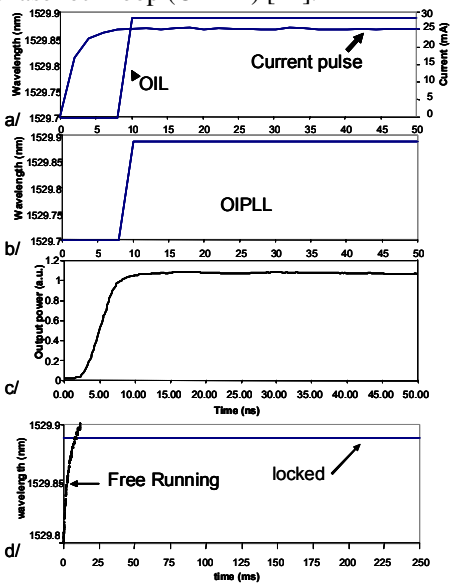

Fig. 2. Channel-switching transient 1570-1529.89 nm (resolution 1pm): Wavelength stabilization is achieved within 10 ns of the onset of the electrical trigger signal (a) with OIPLL (b) with OIL only, whilst the optical output power stabilizes within 10 ns (c). The OIPLL removes any wavelength drift over the 250 ms pulse length (d).

For these experiments the comb source was an amplified fibre loop with embedded phase modulator as in [3]. Its spectrum was delivered to (slave) lasers in OIPLL blocks (combined OIL and OPLL), which were locked to selected lines. Fast and slow channel laser drifts were compensated by the operation of the OIL and OPLL circuits, the two locking techniques in combination allowed increased OPLL loop delay time (27 ns), wide channel laser linewidths (> 10 MHz) and wide locking ranges simultaneously, in contrast to previously implemented stand-alone techniques [12], which only provided 2 GHz locking range compared with the 80 GHz of the OIPLL technique.

Wavelength monitoring was carried out using a preselecting optical bandpass filter followed by a scanning Fabry-Perot interferometer (FPI) tuned by a high-precision (1 mV resolution) digital to analogue converter (DAC), with the FPI output detected using a photodiode and digital storage oscilloscope. Scanning the interferometer as the OIPLL is repetitively switched between wavelengths allows profiles of wavelength and output power to be plotted. An oscilloscope trace was recorded for each voltage/wavelength setting before tuning the FPI by 1 pm (~ 125 MHz). The wavelength range scanned was ≤ 1 nm, limited by the free spectral range of the FPI.

A. Locking Range

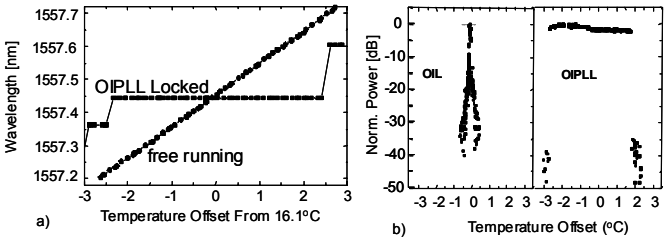

Fig. 3. a) Channel locking as a function of chip temperature through a Fabry-Perot Etalon, b) Power of microwave signal generated by beating two OIPLL (or OIL) locked laser diodes (locked on two consecutive lines; 18 GHz spacing).

Fig. 2a shows the measured locking range in terms of laser temperature measured by FPI. The OIPLL controlled laser was locked (measurement precision is 1 GHz) over a 5 K temperature range. We measured also the side mode suppression ratio (SMSR) with a spectrum analyzer and the output power of the laser. The SMSR remained above 35 dB throughout the locking range. The changes in output power are due to the control loop voltage, which induces up to 40 mA current change in the gain section. It will be sufficient to apply the control voltage to one of the other sections (preferably the phase) to avoid this effect. Furthermore, the range could be increased by applying control signals to the reflector sections [13]. To provide a higher resolution measurement, we used two OIPLL circuits locked to two adjacent lines from the comb generator. By heterodyning the output from the two lasers, we could measure how well the OIPLL is able to maintain spectral spacing and hence how good the locking is (resolution bandwidth of 1 kHz). Fig. 2b shows such a measurement. The highest power occurs only when the lasers emission frequencies are exactly 18 GHz apart (1 kHz precision), showing that locking is maintained to within the measurement limit.

A. Fast Switching

Fig. 3 shows the switching performance for a selected pair of wavelengths: 1570 nm (rear section current: 0 mA) and 1529.89 nm (peak tuning rear section current 25 mA) at a frequency of 1 kHz. The new wavelength is acquired to the system measurement accuracy of < 250 MHz, within 10 ns (Fig. 3b OIL, Fig. 3c OIPLL), for a current pulse of rise time 8 ns (Fig. 3 a). This proves that when the new wavelength is acquired it is effectively locked by the OIPLL (an unlocked channel would show changes >250 MHz) in a time < 5 ns as a current sufficient to tune the laser to within the OIL locking bandwidth is reached after 5 ns. The comparison of acquisition time for OIL and OIPLL (Fig. 3b and Fig. 3c)) demonstrates that the optical injection is the predominant locking mechanism responsible for fast switching time. To complete the measurements we also made a long term stability test by keeping the rear section current at 25 mA and scanning the spectrum over a 250 ms time window (Fig. 3d). The wavelength remained locked and stable during the time window proving that the long term wavelength drift was < 250 MHz (measurement limited). In comparison, the wavelength drift over 5 ms for an unlocked laser is more than 9 GHz [11].

IV. Fast Photodetector

The UTC structure used for this work was designed to offer both relatively high coupling from an optical fibre into the detector and short absorption length to reduce the parasitic capacitance. This resulted in an absorption layer thickness such that the carrier transit limited 3dB bandwidth was about 340 GHz. The length of the device necessary to absorb 90% of the incoming light was calculated to be 15 μm. Considering the characteristics of the structure this will correspond to an 18 fF parasitic capacitance, thus giving a parasitic capacitance limited bandwidth of 350 GHz with a 50 Ω load- of the same order of magnitude as the carrier transit limited 3 dB bandwidth. However, once fabricated the waveguide device was measured to have a capacitance of 20-25 fF, which gives a capacitance limited 3dB bandwidth of 254 GHz with a 50 Ω load, which should be the main limitation on the bandwidth of the detector.

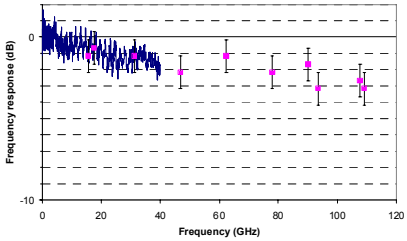

Fig. 4. Relative UTC-PD response up to 110 GHz.

The experimental measurements on the detector were made using two different systems. The first was a Lightwave Component Analyser (LCA), used for studies up to 40 GHz. The output of the LCA is a 10 dBm power level optical signal at 1550 nm. At the end of the lensed fibre this drops to 9 dBm. Then by taking the result of simulation for the coupling into the waveguide we can estimate the coupled power into the photodetector to be 5 dBm. The second measurement system, used a signal from an heterodyne system based on an optical frequency comb generator [3], from which two lines were filtered out by tuneable narrow-band filters. The two lines were then combined and amplified to generate a signal at a frequency determined by their separation. The total saturated output power from the EDFA was 21 dBm, thus the estimated power coupled into the device was 17 dBm. The measured photocurrent at this level of power was 10 mA. However the filters used in this experiment were relatively broad (several comb lines were transmitted) thus the generated signal comprised several beating frequencies. Therefore not all the generated power was at the frequency of interest for the measurement. The resulting signal measured by the probe was then sent to a spectrum analyser. The device was probed with coplanar

probes (one for signals from 0 to 65 GHz using coaxial electrical connection and one for signals from 70 to 110 GHz using waveguide electrical connection). The probes were connected to different calibrated harmonic microwave mixers to down-convert the high frequency signals for display on a spectrum analyzer.

Using the LCA we measured the dependence of bandwidth on reverse bias and the response up to 40 GHz. The optimum bias was -2 V, where the frequency response was flat up to 40 GHz. This showed as well that about 10 μW power could be extracted from the photodiode with the 5 dBm optical excitation. To measure the response at higher frequency the heterodyne system was used. To obtain the relative response of the photodetector up to 110 GHz with -2 V bias, points were taken below 40 GHz with the heterodyne measurement system in order to relate them to the previous measurements. As seen in Fig. 4, the experiment showed that the response remains above -3dB up to 108.2 GHz within the error of the measurement. The mean photocurrent at 110 GHz as a function of the estimated coupled input optical power corresponds to a measured responsivity of 0.2 A/W.

V. Millimeter Wave Heterodyne Generation

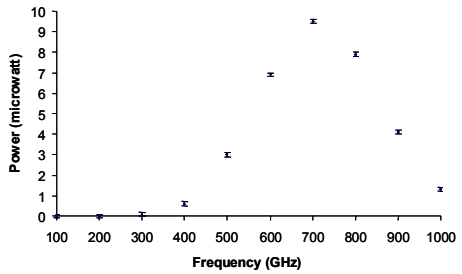

Fig. 5. Signal emitted from the bowtie antenna as a function of the Frequency.

The measurement system used the heterodyne system described above (with high selectivity filters) to generate high spectral purity frequencies from 100 GHz to 1 THz. The optical power sent to the photodiode generated a 10 mA photocurrent. The signal emitted from the integrated antenna (bowtie or resonant) was measured using a THz power meter based on a photo-acoustic detector for powers above 10 μW and a bolometer for power under 10 μW.

Fig. 5 shows the measured extracted THz wave power at different heterodyne frequencies. One can see the response of the broadband antenna resulted in a broadband emission peak around 700 GHz. The maximum extracted power was at 700 GHZ with 9.5 μW and there was still more than 1 μW at 1THz. When the device was integrated with a resonant antenna more power could be extracted but only within a narrow band around the resonant frequency. Two resonant peaks of emission at 457 GHz and 914 GHz were obtained with record breaking power outputs of 148 μW and 24 μW respectively.

VI. Conclusion

By combining telecommunications wavelength device technologies with novel ultra-fast photodetectors, efficient CW THz generation is enabled. Using UTC based detector designs we have achieved CW output powers of over 0.14 mW at 457 GHz and over 0.02 mW at 914 GHz for optical powers of less than 150 mW. Further the THz signals have high spectral purity, limited primarily by the spectral purity of the microwave reference source.

Looking forward we anticipate considerable further advances in detector technology, making efficient photonic generation of CW THz signals possible to frequencies of order 2 THz.

References

[1] www.teraview.co.uk

[2] H. Ito, T. Furata, S. Kodama, T. Ishibashi, "InP/InGaAs uni-travelling-carrier photodiode with 310 GHz bandwidth," Electron. Letters, 36, pp 1809-1810, 2000

[3] N. Shimosaka, K. Kaede, M. Fujiwara, S. Yamazaki, S. Murata, M. Nishio, "Frequency separation locking and synchronization for FDM optical sources using widely frequency tunable laser diodes," Sel. Area Com., vol. 8, pp. 1078-1086, 1990

[4] M. Kourogi, K. Nakagawa, M. Ohtsu, "Wide-span optical frequency comb generator for accurate optical frequency difference measurement," IEEE journal of Quantum Electron., vol. 29, pp. 2693-2701, 1993

[5] S. Bennett, B. Cai, E. Burr, O. Gough, A. J. Seeds, "Terahertz, zero frequency error, tunable optical comb generator for DWDM applications," Paper WM5 OFC'99, San-Diego, 1999

[6] M. Teshima, M. Koga, K. Sato, "Accurate frequency control of a mode-locked laser diode by reference-light injection," Optics Letters, vol. 22, pp. 126-128, 1997

[7] D. J. Kuizenga, A. Siegman, "FM-laser operation of the Nd:YAG laser," IEEE journal of Quantum Electron., vol. 6, pp. 673-677, 1970

[8] B. Cai, A. J. Seeds, J. S. Roberts, "MQW tuned semiconductor lasers with uniform frequency response," IEEE Photonics Technol. Letters, vol. 6, pp. 496-498, 1994

[9] J. B. Songs, C. C. Button, A. J. Seeds, "1.55 μm multichannel DWDM source using quaternary/quaternary MQW InGaAsP/InP QCSE tuning," IEE Electron. Letters, vol. 37, pp. 426-427, 2001

[10] E. J. Skogen, J. W. Raring, J. S. Barton, S. P. DenBaars, L. A. Coldren, "Postgrowth control of the quantum-well band edge for the monolithic integration of widely tunable lasers and electroabsorption modulators," IEEE J. of Selected Topic in Quantum Electron., vol. 9, pp. 1183-1190, 2003

[11] C. F. C. Silva, M. Dueser, V. Mikkhailov, C. C. Renaud, P. Bayvel, A. J. Seeds, "Fast channel hopping, zero frequency error source for high spectral efficiency, dynamic wavelength-routed optical networks," proceedings of CLEO'03, 2003.

[12] L. A. Johansson, A. J. Seeds, "Millimeter-wave modulated optical signal generation with high spectral purity and wide-locking bandwidth using a fiber-integrated optical injection phase-lock loop," IEEE Photon. Technol. Lett., vol. 12, pp. 690 –692, 2000.

[13] C. C. Renaud, M. Fice, I. Lealman, P. Cannard, A. J. Seeds, "100 GHz Spaced 10 Gbit/s WDM over 10 ^{o}C to 70 ^{o}C using an uncooled DBR laser," OFC 2006, Anaheim, 2006